science, engineering and health studies

Research Article

Science, Engineering and Health Studies
https://li01.tci-thaijo.org/index.php/sehs
ISSN (Online): 2630-0087

Application of external horizontal shading slats for daylighting through north-facing windows

Simeon Nyambaka Ingabo[*], *Surapong Chirarattananon and Pipat Chaiwiwatworakul*

The Joint Graduate School of Energy and Environment, CHE Center for Energy Technology and Environment, King Mongkut's University of Technology Thonburi, Bangkok 10140 Thailand

ABSTRACT

Shading slats allow for illumination of indoor spaces by the use of natural daylight while preventing the penetration of undesirable beam solar radiation. Extensive research has been performed on the use of shading slats on south-facing windows in tropical climate. However, studies on the use of this shading device for north-facing windows are rare, owing to the prevailing assumption that they are not beneficial for north-oriented facades at higher latitudes. This study investigated the operation and energy-saving potential of adjustable external horizontal slats installed on north-facing windows of office buildings in a tropical climate. Full-scale experiments were performed and the results were used to validate a simulation model. Simulations were performed to estimate the energy consumption in offices of varying dimensions over a full year. The appropriate slat adjustment angles for each month were determined and total lighting and air conditioning energy savings of up to 50% were estimated in comparison to the use of unshaded windows with heat-reflective glass.

***Corresponding author**:
Simeon Nyambaka Ingabo
simeon.ing@mail.kmutt.ac.th

***Received**: 4 February 2020*
***Revised**: 24 August2020*
***Accepted**: 16 September 2020*
***Published**: 15 January 2021*

***Citation**:
Ingabo, S. N., Chirarattananon, S., and Chaiwiwatworakul, P. (2021). Application of external horizontal shading slats for daylighting through north-facing windows. Science, Engineering and Health Studies, 15, 21040002.*

Keywords: daylighting; external slats; north-facing windows; energy saving

1. INTRODUCTION

Solar shading devices are an integral design component of most buildings in tropical regions. They alter indoor visual and thermal conditions and subsequently influence a building's energy consumption whilst enabling the occupants to control their privacy (O'Brien et al., 2013; Cheng et al., 2007). While the main function of shading devices is to shield buildings from direct solar radiation (Kirimtat et al., 2016), they can also serve other purposes such as space cooling and control of daylighting. Previous studies and literature on external shading devices installed on southern facades greatly outnumber those on northern facades, and thus there is a need for additional studies on the latter case.

The energy-saving potential of shading devices installed on south-facing windows has been studied extensively at high latitudes since the sun appears in front of southern facades for most of the year. Reductions in energy consumption of 30% to 70% have been found (Tzempelikos and Athienitis, 2007; Nielsen et al., 2011; Li and Tsang, 2008). Hammad et al. (2010) studied the impact of automated external louvers on an office building's overall energy consumption in the United Arab Emirates. Simulations were performed using the Integrated Environmental Solutions Virtual Environment software (IESVE) with dimmable lighting incorporated. Lighting and air-conditioning energy consumption were analyzed. The study showed that, depending on window orientation, energy savings of 29% to 34% were attainable. Another simulation study by González and Fiorito (2015) utilized the Rhinoceros program to optimize energy efficiency and

the visual comfort of external shading, showing enhanced energy efficiency and comfort.

The effectiveness of a shading device is dependent on numerous factors. Datta (2001) evaluated the performance of external fixed shading louvers on the southern facade in four different cities and established that the tilt angle, slat dimensions, and distance between slats are critical when evaluating heat gain or energy. The study also concluded that each location had its own specific suitable shading configuration. Alzoubi and Al-Zoubi (2010) examined light distribution in an office in Jordan with fixed external shading slats on the south-oriented facade. Simulations were performed using Lightscape to determine illuminance at different work plane points and on the walls of the office. Comparisons were made to a reference case of an unshaded window and it was observed that interior daylight distribution for unshaded windows was homogenous, while rooms with shaded windows had better spatial visual quality since shading slats could alter daylight distribution depending on the tilt angle. Slat properties such as slat separation distance, slat length, and slat material also affect energy savings, daylighting, and thermal performance (Stazi et al., 2014).

Besides their energy-saving potential, adjustable shading devices have the additional advantage that they can adopt to changing outdoor conditions and are therefore preferred over fixed shading devices (Yao et al., 2016). Aste et al. (2012) compared the performance of an adjustable external venetian blind system with that of an electrochromic glazing system on a test cell assumed to be part of an office building. They established that the electrochromic glazing system performed better than external venetian blinds in terms of primary energy consumption; however, installation costs were excessive, thus making the external venetian blind system a better intermediate option.

Regarding north-facing windows in tropical climates, Chaiwiwatworakul et al. (2016) examined the daylighting and heat-transfer performance of shading slats located between two glazed panes for both south and north windows. Daylighting and heat-transfer models were developed and experiments and simulations were performed. They observed significant overall energy savings up to 50% for north-facing windows. Similar research focused on external slats and shading devices on north-facing windows at high latitudes is uncommon since the sun is either overhead or incident on southern facades for most of the year; thus, direct incident solar radiation is absent. However, diffuse radiation and daylight are still quite abundant and can also affect a building's overall lighting and cooling energy consumption.

This paper sought to justify the use of external shading slats for north-facing windows by estimating their energy-saving potential and effective adjustment. Full-year optimum slat adjustment schemes and lighting and cooling energy consumption were examined for monthly adjusted external horizontal slats installed on north-facing windows of office buildings in a tropical climate. Experiments were conducted in a full-scale room to measure indoor daylight distribution and thermal transfer through the shaded window. The calculation program BESim was validated using the experimental results. Full-year simulations were performed using the validated program to compare monthly adjustment angles and energy consumption to the use of windows with heat-reflective (HR) glass with no shading. Energy savings from the use of this device for office spaces of varying dimensions with north-facing windows were also estimated.

2. MATERIALS AND METHODS

2.1 Experiments

Experiments were performed on different days to measure daylight from a north-facing window with manually adjusted external slats. The full-scale experimental room and setup are shown in Figure 1. The room was located on the rooftop of the School of Bio-resources and Technology building at the Bang Khun Tien campus of King Mongkut's University of Technology Thonburi (latitude 13.70°N and longitude 100.44°E). The room has a length of 9 m, a width of 3 m, and a floor-to-ceiling height of 2.65 m with a north-facing window of a height of 1.80 m and a width of 2.70 m. The window sill was 0.85 m above the floor. The ceiling and floor reflectance values were 0.7 and 0.3, respectively. White horizontal slats made from aluminum were installed outside the window. The slat width and separation were 0.13 m and 0.10 m, respectively. The room was air-conditioned by a fan coil unit. Properties of the materials used are shown in Table 1.

(a) Exterior view of the experimental room

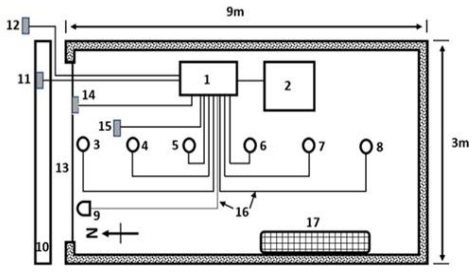

Key			
1	Data logger	10	External slats
2	Computer	11	Pt 100 sensor to measure slat temp.
3	Luxmeter to measure transmitted daylight	12	Pt 100 sensor to measure outdoor temp.
4	Luxmeter to measure work plane daylight at 10% depth	13	Glazed window
5	Luxmeter to measure work plane daylight at 30% depth	14	Pt 100 sensor to measure glazing temp.
6	Luxmeter to measure work plane daylight at 50% depth	15	Pt 100 sensor to measure indoor temp.
7	Luxmeter to measure work plane daylight at 70% depth	16	Connecting cables
8	Luxmeter to measure work plane daylight at 90% depth	17	Fan coil unit
9	Pyranometer to measure transmitted solar radiation		

(b) Experimental setup

Figure 1. Experimental site and setup

Table 1. Properties of the materials used

Specifications	Materials			
	Slat	Clear glass	Heat-reflective glass	Opaque wall
Material	Aluminum	Glass	Glass	Lightweight concrete
Density (kg/m^3)	2710	2512	2500	620
Thickness (m)	0.002	0.006	0.012	0.1
Conductivity (W/m.K)	205	1.05	1.05	0.16
Specific heat capacity (kJ/kgK)	920	880	840	840
Visible reflectance	0.8	0.08	0.32	0.7
Visible transmittance	0	0.88	0.09	0
Solar reflectance	0.8	0.07	0.33	0.7
Solar transmittance	0	0.8	0.06	0

Slat tilt angles of 0° (fully opened slats) and 40° (tilted downwards) were considered for the experiments. Work plane daylight was measured using light sensors installed at 10%, 30%, 50%, 70%, and 90% of the depth along the center of the experimental room. The temperatures of the slats, outdoor air, indoor air, and glazed pane were measured using Platinum RTD (Pt100) sensors. The transmitted daylight and solar radiation through the shaded window were also measured using a light sensor (Model ML-020S-O supplied by Eko Instruments, Japan) and pyranometer (Model CMP10 supplied by Kipp & Zonen, Nethelands), respectively. Minute-by-minute measured data were recorded by a data acquisition system comprising a data logger and a computer for office hours from 8:00am to 5:00pm. An unobstructed meteorological station located at the same campus simultaneously recorded the beam, diffuse horizontal and global daylight illuminance, and the solar irradiance. The vertical solar irradiance and daylight in the northern, eastern, southern, and western orientations and the ambient air humidity and temperature were also measured by the station.

2.2 Calculations

The simulation program BESim, validated by Chaiwiwatworakul et al. (2012) and Chirarattananon and Hien (2011), was used to calculate indoor daylight in a model office room with a north-facing shaded window with adjustable external slats. The program uses data from the meteorological station to perform thermal and daylight calculations based on the method examined by Hien and Chirarattananon (2005). The illuminance calculations utilize configuration factors, raytracing, and flux transfer and were based on the ASRC-CIE sky model (Perez et al., 1990). Figure 2 shows the incremental illuminance from a patch of sky transmitted through a shaded window. The incremental illuminance was calculated using Eq. 1, where dEk represents the incremental illuminance transmitted through the glazed window from a sky patch (lux), τ is the transmittance of the glazing, L(γ,ϕ,ξ) is the sky luminance at a particular position (cd/m^2), γ and ϕ are positional angular variables related to the sky patch, and ξ is the angular distance between the sun and the patch. The program calculates heat transfer using the finite-difference method and energy balance principles.

$$dEk = \tau L(\gamma, \phi, \xi)\sin\phi\cos\phi d\phi d\gamma. \quad (1)$$

A rectangular model room, as shown in Figure 3, with similar dimensions to the experimental room was chosen to outline the energy calculation process. It had a shaded window on the northern wall. The room surfaces and materials had similar properties to those of the experimental room, as shown in Table 1. Weather data recorded over an entire year was used to calculate hourly work plane daylight (at 10%, 30%, 50%, 70%, and 90% room depths) and transmitted radiation for each day of the year between working hours. Supplementary light from dimmable lamps required to meet the target work plane illuminance and the air-conditioning energy consumption were calculated for cases when the slats completely shaded beam radiation. Energy savings were estimated in comparison to the typical case of windows with unshaded HR glass.

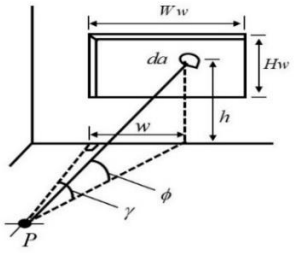

Figure 2. Incremental illuminance from a patch of sky at an interior point

2.3 Electric lighting and air-conditioning energy

It was assumed that dimmable LED lamps were installed uniformly on the ceiling of the model room to supplement natural daylight when necessary in order to achieve a uniform target work plane illuminance of 500 lux. The lighting power density (LPD) determined by the IESNA lumen method was found to be 10.58 W/m^2 for a target work plane illuminance of 500 lux, as indicated in Table 2. Indoor air temperature was maintained at 25°C by an air-conditioning unit with a coefficient of performance (COP) of 2.8. Cooling load calculations considered convective heat from the shaded window and the opaque section of the wall below the window, transmitted solar radiation, and heat from electric lamps. It was postulated that the cooling load from the lamps was equal to the heat produced by the electric lamps.

The total cooling energy consumption by the model room En (kWh/year) was calculated using:

$$En = \left(LPD + \frac{LPD + HG(A_w/A_f)}{COP}\right) A_f H, \quad (2)$$

where LPD represents average lighting power density (W/m$_{fl}^2$), HG represents total heat gain from the windowed-wall (W/m$_w^2$), COP represents the coefficient of performance, and A_w and A_f are the areas of the windowed wall and floor area (m^2), respectively, while H represents the total annual office working hours (2340 h).

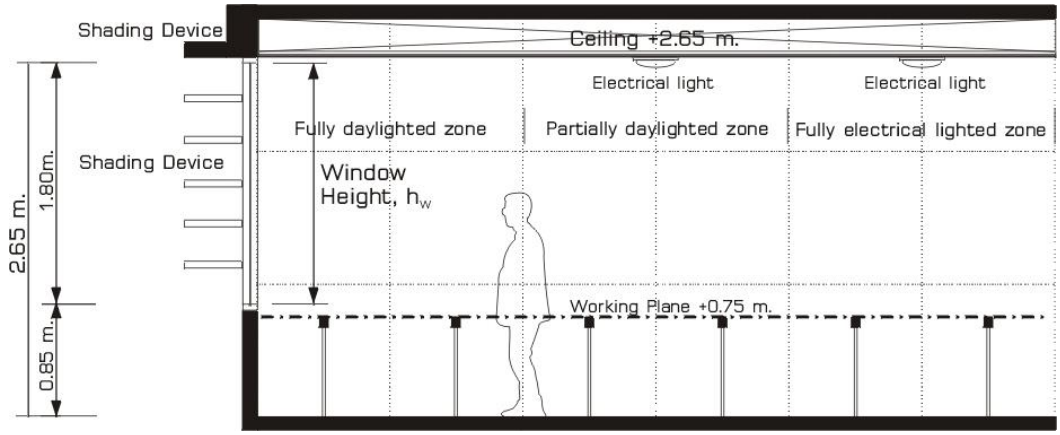

Figure 3. The model room

Table 2. Details of the lighting system

Parameter		
Number of lamps per luminaire	2	$E_w = (LLF)(CU)(\frac{Lf}{P})(\frac{P}{A})$
Total light flux (lm)	5360	
Total power (W)	58.9	
Efficacy (lm/W)	90.9	
Work plane illuminance (lux)	500	
Lighting power density (W/m^2)	10.58	

Note: E_w target workplace illuminance (lux)
LLF light loss factor (0.8)
CU coefficient of utilization (0.65)
Lf/P efficacy (lm/W)
P/A lighting power density (W/m^2)

2.4 Daylighting schemes

Three daylighting schemes were examined to compare the energy consumption behavior of the selected model room. Each scheme was required to meet the minimum condition of preventing penetration of direct solar radiation during working hours, which was determined as outlined by Chaiwiwatworakul et al. (2016) using the proportion of the glazing area exposed to sunlight to the total glazing area F_b.

Figure 4 illustrates the cases of fully shaded and partially shaded direct solar radiation, with Eqs. (3), (4), and (5) used to calculate the values for different slat tilt angles:

$$F_b = 1 - \frac{W_l - \sin\varphi_l}{S_l} - \frac{W_l \cos\varphi_l \tan\varphi_s}{S_l}, \text{ where } \varphi_l \geq 0^\circ, \quad (3)$$

$$F_b = 1 - \frac{W_l - \sin|\varphi_l|}{S_l} - \frac{W_l \cos|\varphi_l| \tan\varphi_s}{S_l}, \text{ where } \varphi_l \geq 0^\circ \text{and } \varphi_s < |\varphi_l|; \text{ and} \quad (4)$$

$$F_b = 1 + \frac{W_l - \sin|\varphi_l|}{S_l} - \frac{W_l \cos|\varphi_l| \tan\varphi_s}{S_l}, \text{ where } \varphi_l < 0^\circ \text{and } \varphi_s > |\varphi_l|, \quad (5)$$

where W_l represents the slat width; S_l is the slat separation distance; φ_s is the solar profile angle; and φ_l is the slat tilt angle. The F_b value must be zero for the entire month in order for a given slat angle to completely shade beam solar radiation for that month.

In the first scheme, the slats were maintained at a fixed angle to only block direct solar radiation as outlined for the whole year, representing typical shading systems. This scheme is referred to as the fixed slats scheme. In the second scheme, the slats were adjusted each month to block direct solar radiation and provide a maximum outdoor view in the horizontal direction. This scheme is referred to as the maximum view scheme. In the third scheme, the slats were adjusted to both block beam solar radiation and to minimize energy consumption by electric lamps and air-conditioning. The slat angle that blocked direct sunlight for the entire month and allowed the most daylight to supplement artificial lighting when necessary was selected. This scheme is referred to as the minimum energy scheme. This procedure was replicated for forty-five different workspaces with varying room depths (D), widths (W), and window-to-wall ratios (WWR), and with identical properties to the model room. To examine the effect of varying room dimensions on interior daylight, the width of the windowed-wall was varied between 3 m, 9 m, and 15 m. The depth of the room from the windowed-wall to the rear wall was also varied between 3 m, 6 m, 9 m, 12 m, and 15 m. WWRs of 0.3, 0.6, and 0.9 were considered.

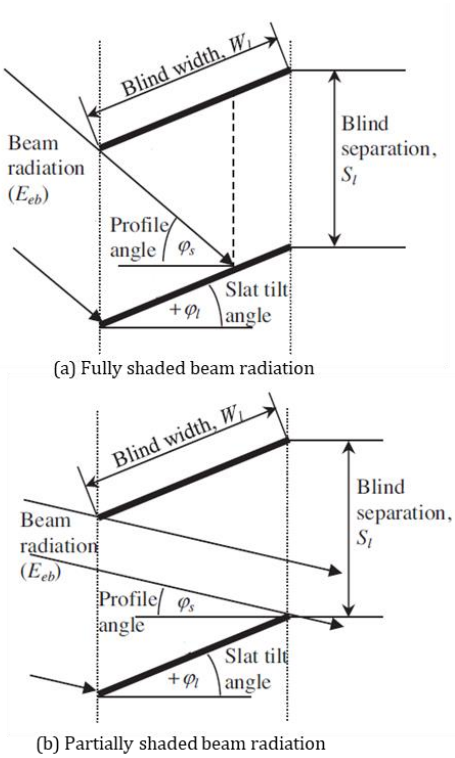

Figure 4. Incident beam radiation on a shaded window

3. RESULTS AND DISCUSSION

3.1 Experimental results

Experiments were conducted for the north-facing window with external slats. The measurements were performed in May and July when the sun was in front of the window with a high elevation angle. Figure 5 shows the experimental results for fully opened slats at 0°. For the selected day (May 18, 2018), the sky was cloudy and quite bright with intermittent beam radiation. The diffuse daylight illuminance from the sky contributed a major component of the global daylight. The daylight on the north facade was as high as 35 klux (9:40 and 14:10), yet was also as low as 10 klux (10:40), owing to the variation in cloud conditions. It was noted that the work plane daylight near the north window (10%D and 30%D) was high and needed additional shading for proper daylight control. Figure 5(d) illustrates that the daylight near the rear wall was also sufficiently high for general lighting. For the thermal performance, the window reduced transmitted solar irradiance by more than 50% of the total vertical irradiance. The interception of the beam irradiance reduced the absorption of solar radiation by the glazing, thus lowering the temperature. In this experiment, the room was air-conditioned using a fan coil unit. The glazed pane temperature varied between 26°C and 30°C, which was lower than the ambient temperature.

Another experiment was conducted on July 19, 2018. The slats were tilted downwards at 40°. The measured results are shown in Figure 6. On this day, the exterior daylight and solar irradiance were largely variable with a dominant diffuse component (Figure 6(a) and (b)). Figure 6(c) shows that extensive shading of the sun's rays reduced the transmitted daylight and offered a better interior daylight environment. However, the length of time in which the illuminance at great depths into the room (90%D) was lower than 100 lux increased compared to that of the previous experiment.

In the experimental study, the measured surface temperatures, daylight, and solar irradiance were compared with the results of the simulation using the BESim calculation program. The measured and calculated results had matching trends for both experiments and were consistent as shown by the mean bias difference (MBD) and root-mean-square difference (RMSD) values indicated in Table 3 and calculated using Eqs. (6) and (7), respectively:

$$MBD = \frac{1}{N} + \sum_{i=1}^{N}(C_i - M_i) \text{ and} \quad (6)$$

$$RMSD = \frac{1}{N}\sqrt{\sum_{i=1}^{N}(C_i - M_i)^2}, \quad (7)$$

where C_i is the calculated value from the simulation program, M_i is the corresponding measured value from the experiment, and N is the number of considered data points. However, the calculation program overestimates work plane illuminance at 10% depth for fully open slats at 0°.

3.2 Simulation results

The validated BESim program was used to calculate indoor daylight and associated heat gains from the aforementioned adjustment schemes of the external horizontal slats. Annual hourly records of the solar irradiance and outdoor daylight recorded by the meteorological station were used for the calculations.

3.2.1 Model room

Figure 7 shows the slat adjustment angles determined for the three schemes. For the fixed slats scheme, the slats remained fully opened at 0° all year, as it was determined that fully opened slats could shade direct sunlight for the entire year as indicated by the F_b values in Table 4. The slat tilt angles of the fixed scheme were established to be similar to those of the maximum view scheme since fully opened slats also provided an unobstructed view of outdoor surroundings. Daylight simulations were performed for all angles between −30° and 40° to determine optimum slat angles for the minimum energy scheme. Beam solar radiation could not penetrate through the slats all year for all slat angles, except when slats were tilted upwards at −30° from May to July, as seen in Table 4. The energy consumption for all angles that could shade beam radiation was calculated using Eq. 2, and the angle that yielded the least energy consumption was selected for each month. In this scheme, it was determined that the slats should be set at 0° (fully opened) from April to August when the sun appears in front of the window at a high elevation. The slats were then tilted upwards at −10° from September to March to introduce more daylight when the sun was either overhead or moving southwards and to save more lighting energy.

3.2.2 Transmitted and work plane daylight

Figure 8(a) shows the monthly average global, diffuse, and beam components of the daylight illuminance on the north facade. The total daylight during normal office hours (8:00-17:00) was 12-22 klux between May and August

when the sun travelled northwards. This value decreased in the remaining months to as low as 8 klux in December. The lower value was due to the absence of the beam component on the north facade from September to April. Since the determined slat adjustment angles were between 0° and −10° for the three schemes, the differences in daylight and heat transfer results were minor and could be neglected. The minimum energy scheme was thus selected for further analysis.

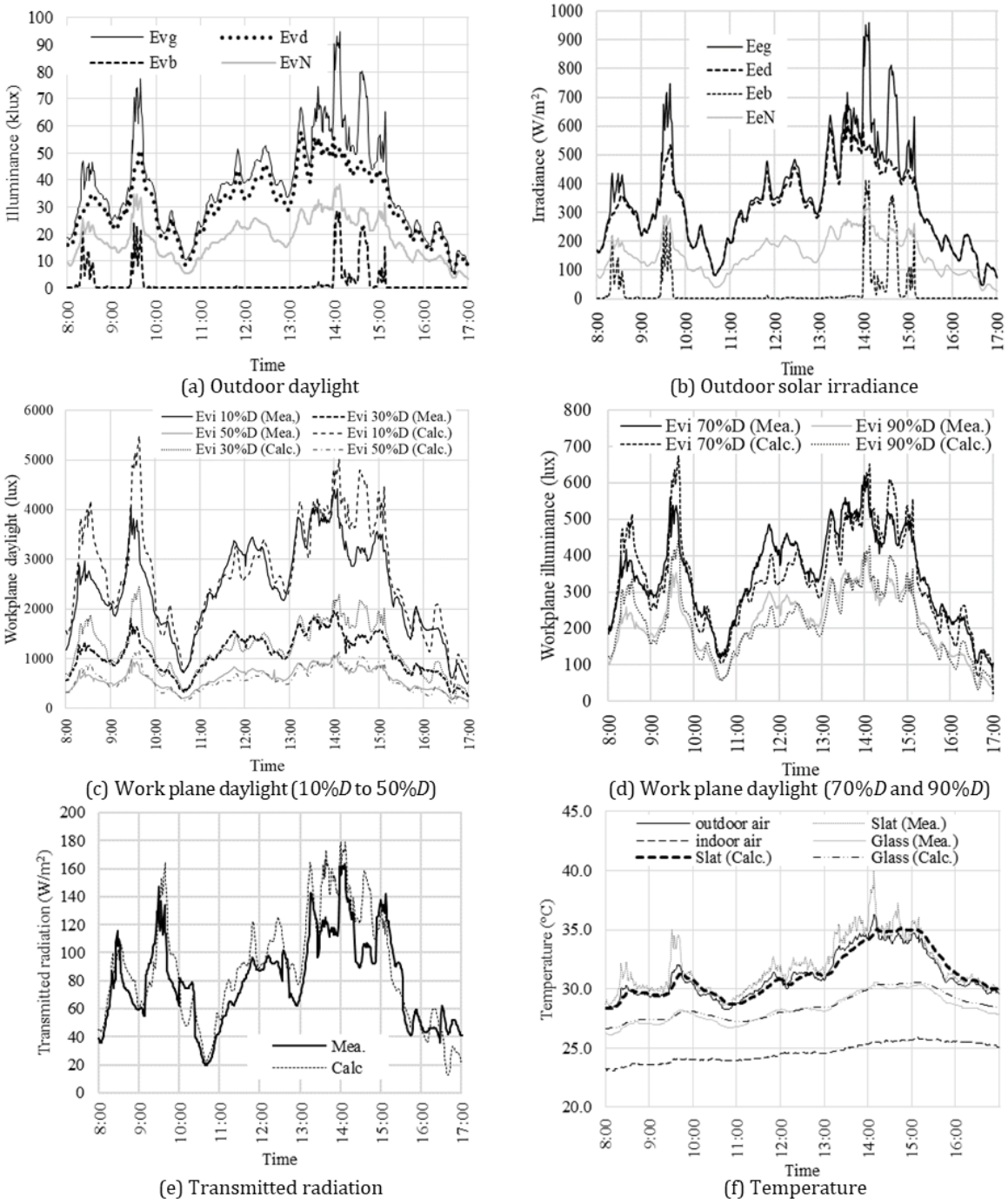

Figure 5. Experimental results for daylight from a north window with slats at 0°

In Figure 8(b), the transmitted daylight for the external slats ranged from 5-13 klux. The slats moderated the large variations in exterior daylight. Despite the window being shaded, the amount of transmitted daylight was close to exterior diffuse daylight due to inter-slat reflection. In comparison to the unshaded window with HR glass, the window with external horizontal slats transmitted at least five times more natural daylight.

Interior illumination was examined based on work plane illuminance. Figure 9 depicts the monthly average maximum values, average mean values, and average minimum values of the work plane daylight. The room

depth/window height ratios (D/H) shown represented the five points on the work plane in the selected model room. The average work plane daylight was observed to be as high as 3,600 lux at D/H = 0.5 near the window in June when the sun appears northwards with a high elevation angle. The maximum average and minimum average reached 5,000 lux and 1,100 lux, respectively, when the slats were fully open at 0°. In December, the average work plane daylight dropped to as low as 2000 lux at D/H = 0.5.

Three zones were identified along the depth of the daylit room. The first zone was the fully daylighted zone where daylight was sufficient to meet the minimum target work plane illuminance of 500 lux. This zone extended from the windowed-wall to D/H = 1.5. However, excessive daylight was observed, implying the need for extra local shading for workstations in this zone. The second zone was the partially daylighted zone, extending from D/H = 1.5 to D/H = 3.5. Work plane daylight in this zone varied between 100 and 2,500 lux. This zone experienced periods when daylight was insufficient to meet the 500 lux requirement, therefore necessitating supplementary artificial lighting. The third zone was the fully daylighted zone, which extended deeper into the space from D/H = 3.5. The average maximum work plane daylight in this zone was below 500 lux for most of the day, and thus electric lighting was required throughout this zone.

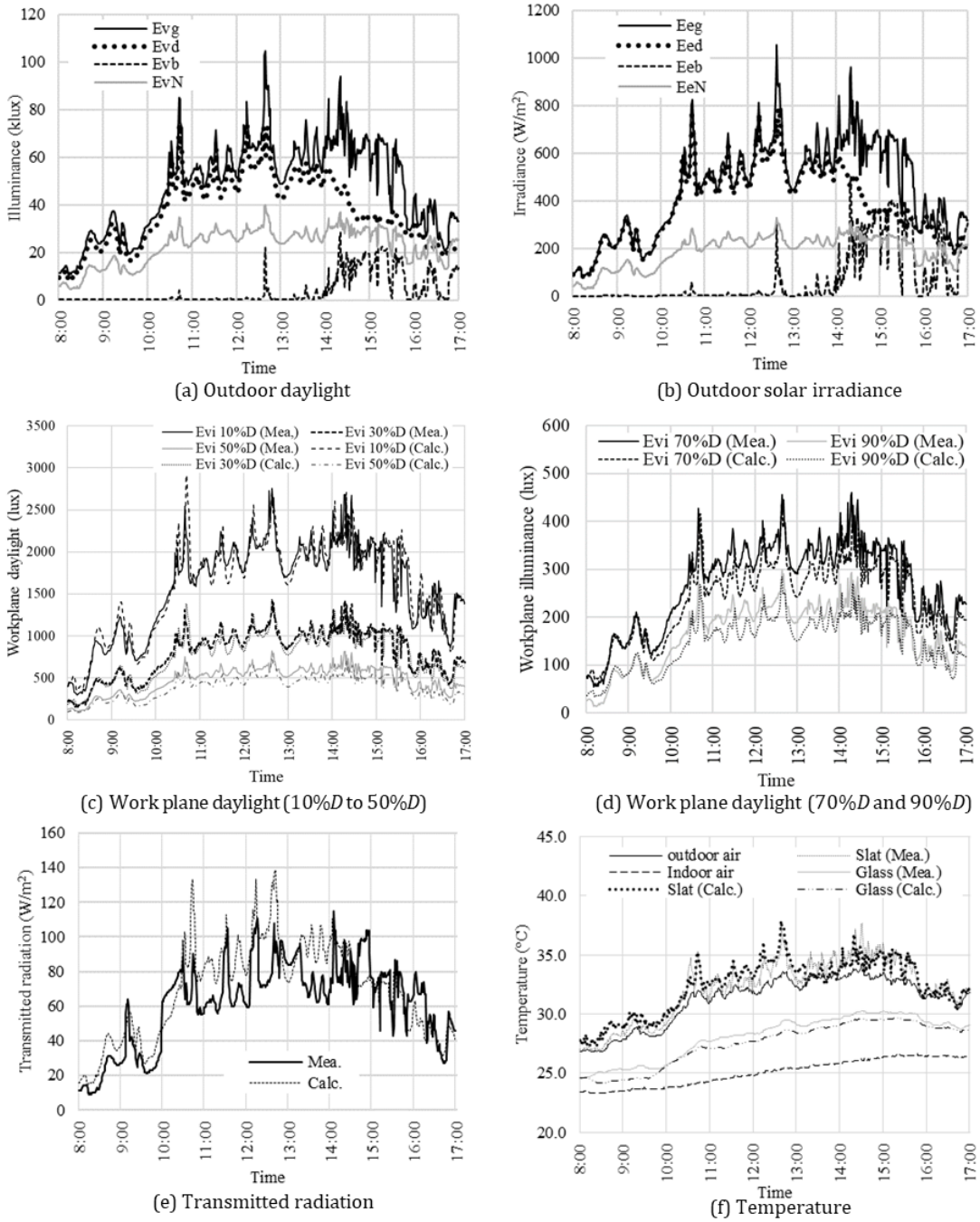

Figure 6. Experimental results of the north window with the slats at 40° (July 19, 2018)

Table 3. RMSD and MBD between the experimental measurements and corresponding calculation values

Slat angle	Evaluator	E_{eT} (W/m²)	$E_{vi\ (10\%\ D)}$ (lux)	$E_{vi\ (50\%\ D)}$ (lux)	$E_{vi\ (90\%\ D)}$ (lux)	T_s (°C)	T_g (°C)
0°	RMSD	0.85	23.37	4.24	1.99	0.70	0.57
	MBD	7.93	863.17	−22.44	−29.97	−0.67	0.61
40°	RMSD	0.76	8.14	4.18	2.08	0.63	0.71
	MBD	7.48	23.58	−80.13	−42.60	0.88	−1.07

Table 4. F_b values for slats at different angles

Angle	F_b values											
	Jan	Feb	Mar	Apr	May	Jun	Jul	Aug	Sep	Oct	Nov	Dec
0°	0	0	0	0	0	0	0	0	0	0	0	0
10°	0	0	0	0	0	0	0	0	0	0	0	0
20°	0	0	0	0	0	0	0	0	0	0	0	0
30°	0	0	0	0	0	0	0	0	0	0	0	0
40°	0	0	0	0	0	0	0	0	0	0	0	0
50°	0	0	0	0	0	0	0	0	0	0	0	0
−10°	0	0	0	0	0	0	0	0	0	0	0	0
−20°	0	0	0	0	0	0	0	0	0	0	0	0
−30°	0	0	0	0	0.223	0.270	0.201	0	0	0	0	0

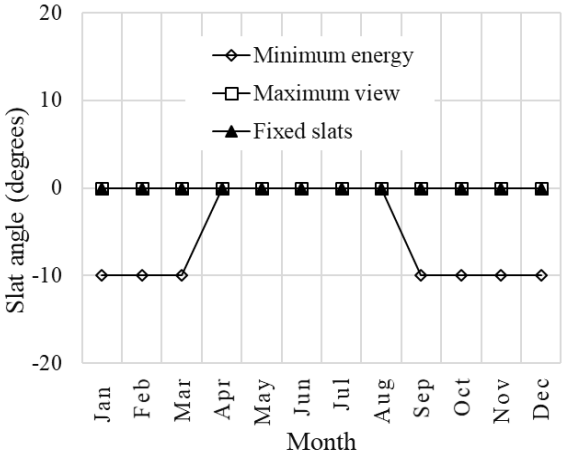

Figure 7. Slat angles for the slat adjustment schemes

3.2.3 Solar thermal gains

The electric energy required for cooling is determined by solar and thermal gains from the shaded window. In this study, the cooling load consisted of dissipated heat from electric lighting and thermal loads from the window and opaque wall sections. Figures 10(a) and (b) depict the vertical solar irradiance on the north plane and transmitted solar radiation, respectively, according to the minimum energy scheme. The observed trends were similar to the associated daylight illuminances in Figure 8.

The total thermal loads shown in Figure 10(c) and (d) were calculated monthly, excluding weekends. The thermal load for the clear glass window with adjustable slats (minimum energy scheme) was observed to be slightly lower than that of the window with HR glass. The transmitted solar radiation contributed the largest share of the thermal load, thus highlighting the necessity of sun shading in the tropics. The thermal load from lighting was reduced by half as compared to the window with HR glass as a result of more daylight penetration and reduced electric lighting consumption.

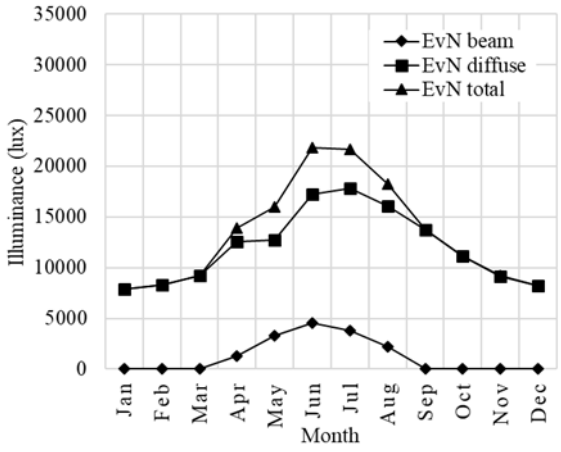

(a) Daylight on the north window

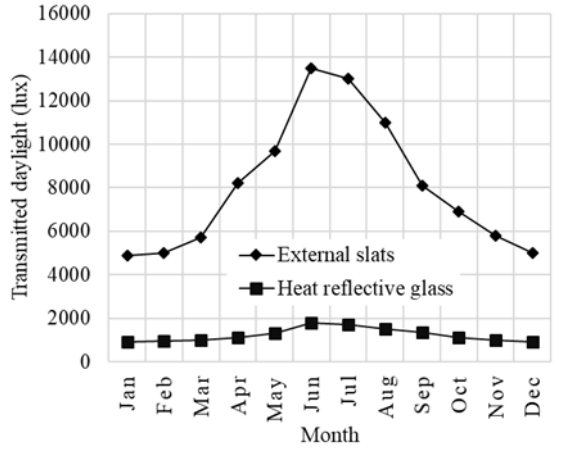

(b) Transmitted daylight

Figure 8. Slat adjustment schemes and daylight illuminance on the north facade

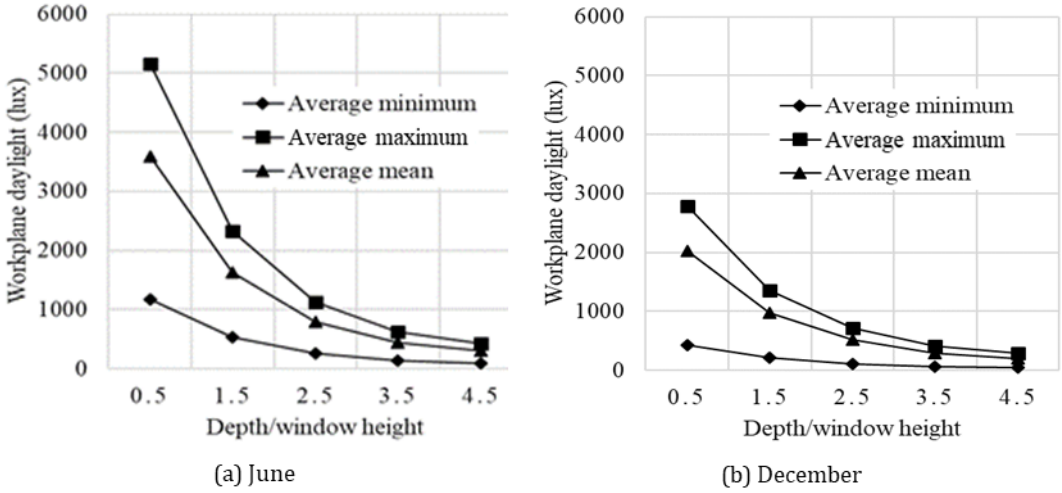

Figure 9. Work plane daylight in June and December

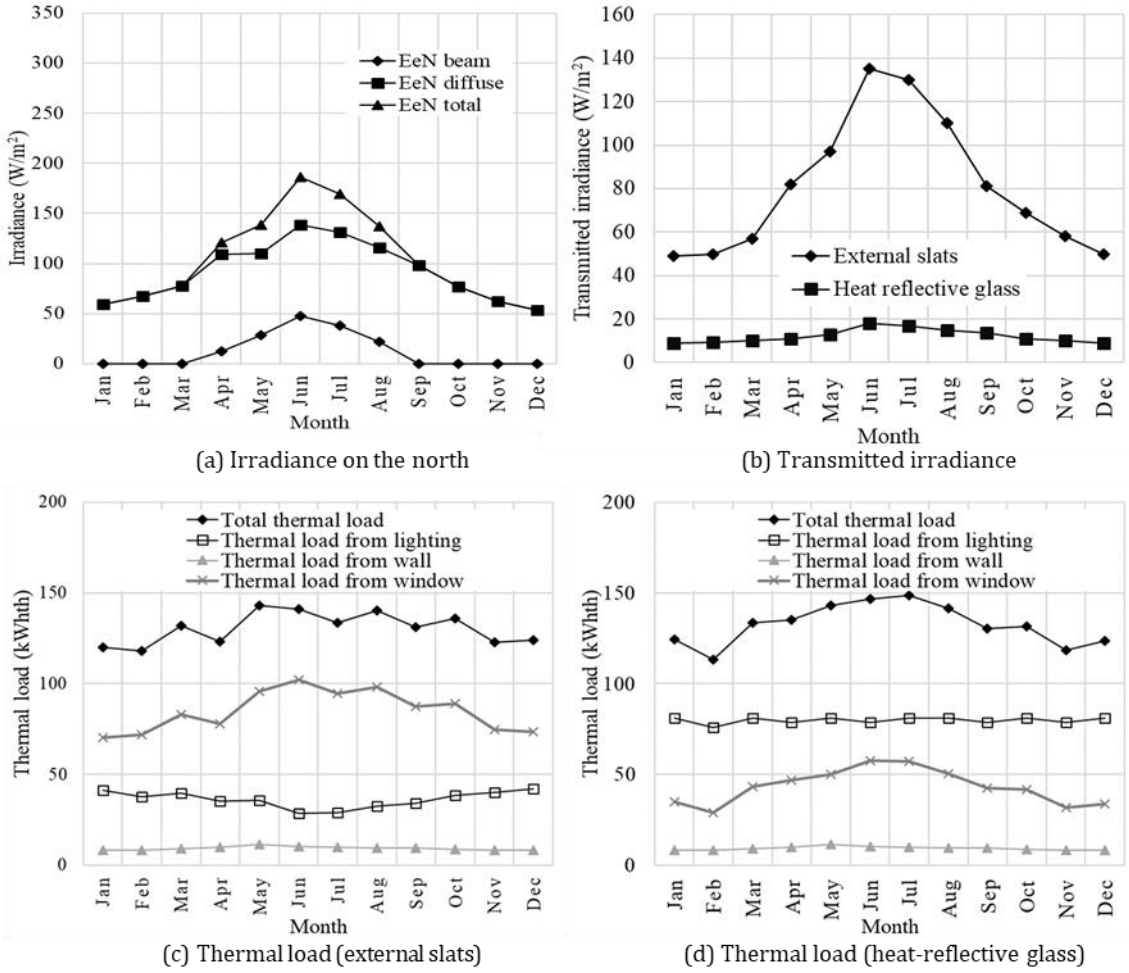

Figure 10. Solar and thermal gains from daylighting

3.2.4 Energy consumption

An assumption was made that the dimmable electric lamps provided a uniform illuminance of 500 lux on the work plane level (0.75 m) with the specific luminaire information shown in Table 2. The average LPD for a target work plane illuminance of 500 lux in June is shown in Figure 11(a). The LPD for slats adjusted under the minimum energy consumption scheme was lower than that of the window with HR glass, owing to the lamps in the latter case being turned on throughout office working

hours. Adjustable external slats allow the penetration of more daylight than HR glass. The lighting energy consumption is shown in Figure 11(b). It was as low as 30 kWh in June for the window with external slats (ES) when the sun was in front of the north window, and increased to 40 kWh during the months when the sun travelled southwards because of reduced daylight penetration. The room with HR glass consumed twice as much lighting energy as the room with external slats.

Cooling energy was determined by the sum of heat and solar gains from electric lighting, the shaded window, and the opaque sections of the north-facing windowed-wall. A COP of 2.8 was assumed for the air-conditioning unit. Figure 11(b) shows the monthly cooling energy consumption. The cooling energy consumption for the window with adjustable external slats was comparable to the case with unshaded HR glass at 40 to 42 kWh in January, increasing up to 58 kWh in June and July during the sun-facing period. While the HR glass reduced the penetration of beam radiation, it resulted in high lighting energy consumption. In contrast, external slats allowed for the penetration of more natural daylight, thus reducing the lighting energy consumption while transmitting more solar radiation than the HR glass, resulting in a comparatively similar overall cooling energy consumption for both cases. Lighting energy was the main portion of total energy requirements. Regardless of the comparable cooling energy consumption, the room with external slats consumed less lighting energy and thus had a lower resultant total energy consumption than the room with HR glass.

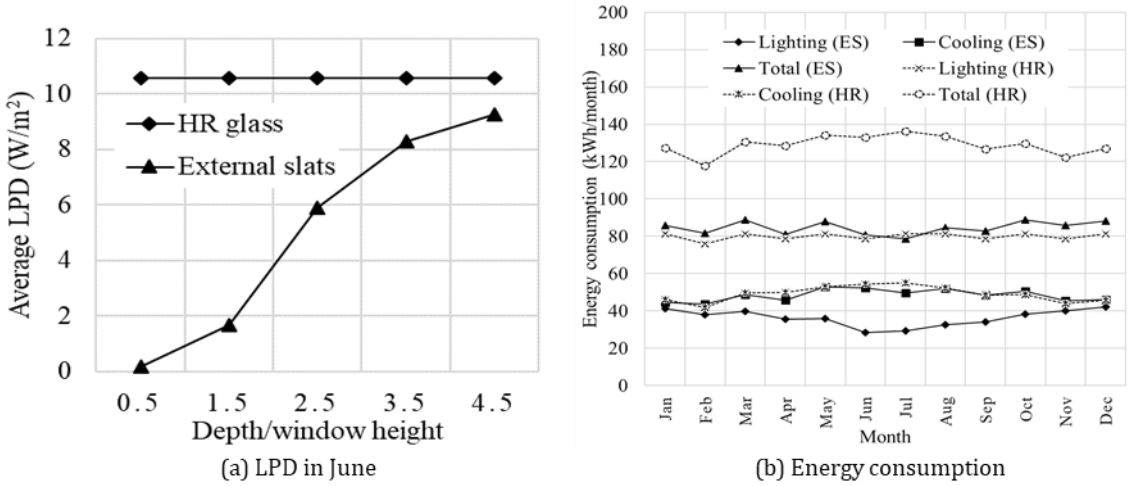

(a) LPD in June

(b) Energy consumption

Figure 11. LPD and energy consumption

3.3 Rooms of varying dimensions

A similar simulation procedure was performed to determine the slat adjustment schedules that minimized energy consumption for rooms with varying depth (*D*), width (*W*), and WWRs, representing the variable nature of office spaces. A target work plane illuminance of 500 lux was maintained. The appropriate slat adjustment angles for each case are shown in Figure 12. It was found that the adjustment schedules were identical for all rooms with depths exceeding 3.0 m. The slats were set at 0° from April to August to block direct sunlight and at −10° for the remaining months to introduce more daylight. The steeper angles observed between April and November for rooms with a depth of 3.0 m could still allow ample daylight, owing to the shallowness of the rooms. However, the differences in energy consumption were minimal for angles ranging from 0° to 20°, and thus a uniform adjustment schedule could be adopted in all studied cases for easier operation.

Figure 13 shows the annual cooling and lighting energy consumption of rooms with varying dimensions. As can be observed, the rooms using daylight from the window with external slats consumed less energy than the rooms with HR glass. Increasing the room width and depth increased the total energy consumption, as more supplementary lighting energy was required. The highest energy savings (40% to 50%) were observed for rooms with depths ranging from 6 m to 12 m.

Larger rooms generally consumed more energy, yet also saved more energy than smaller rooms. Increasing the WWR from 0.6 to 0.9 did not significantly improve energy savings or benefit from daylighting, as the resultant increase in heat gain was greater than additional daylight illuminance on the work plane.

4. CONCLUSION

This study addressed the scarcity of research on daylighting from north-facing windows in tropical climates. The performance and control of external horizontal shading slats installed on north-facing windows was investigated. Appropriate adjustment angles to minimize energy were determined to be 0° from April to August and −10° for the rest of the year. For easy operation, external slats on north-facing windows at this location could be fixed at 0° for the entire year without a significant reduction in energy savings. Office rooms of different dimensions with north-facing shaded windows consumed as much as 50% less energy as those equipped with unshaded heat-reflective glass. External shading slats installed on north-facing windows were found to be just as beneficial as on south-facing windows and are a practically viable replacement for heat-reflective glass.

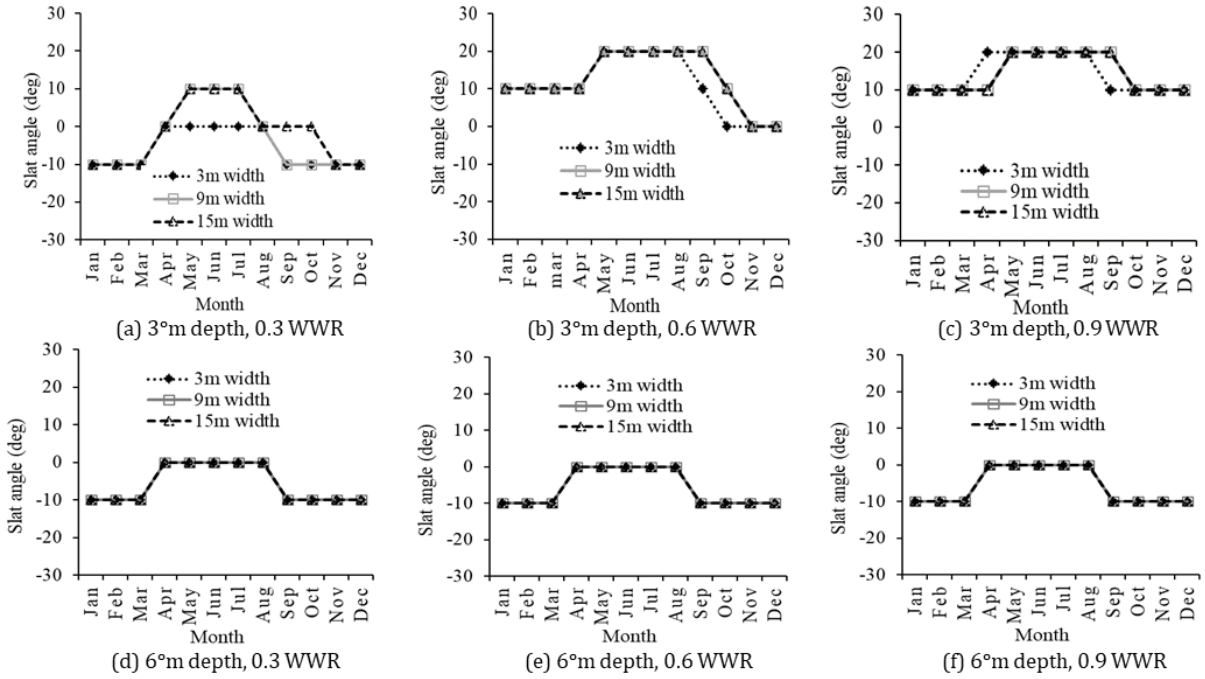

Figure 12. Monthly slat adjustment angles for rooms with varying geometry

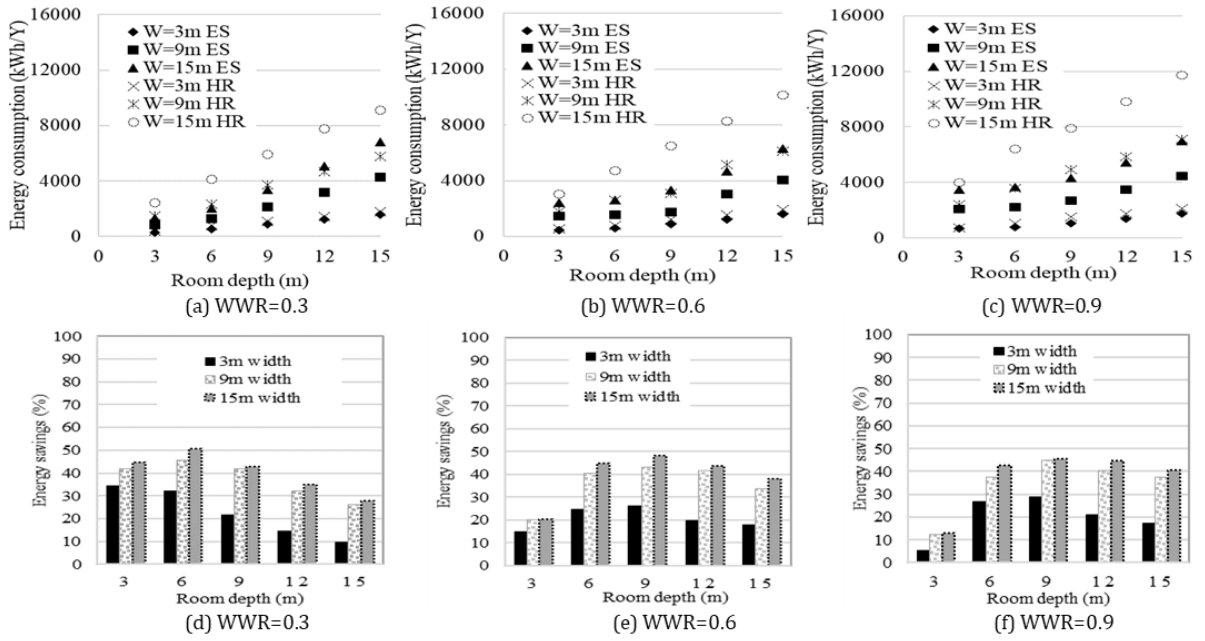

Figure 13. Total energy consumption and energy savings for rooms with varying geometry

REFERENCES

Alzoubi, H. H., and Al-Zoubi, A. H. (2010). Assessment of building façade performance in terms of daylighting and the associated energy consumption in architectural spaces: vertical and horizontal shading devices for southern exposure facades. *Energy Conversion and Management*, 51(8), 1592-1599.

Aste, N., Compostella, J., and Mazzon, M. (2012). Comparative energy and economic performance analysis of an electrochromic window and automated external venetian blind. *Energy Procedia*, 30, 404-413.

Chaiwiwatworakul, P., Chirarattananon, S., and Matuampunwong, D. (2012). Energy saving potential from daylighting through external multiple-slat shaded window in the tropics. *International Journal of*

Renewable Energy Research, 2(3), 376-383.

Chaiwiwatworakul, P., Mettanant, V., and Fathoni, A. M. (2016). Energy analysis of the daylighting from a double-pane glazed window with enclosed horizontal slats in the tropics. *Energy and Buildings*, 128, 413-430.

Cheng, C. L., Chen, C. L., Chou, C. P., and Chan, C. Y. (2007). A mini-scale modeling approach to natural daylight utilization in building design. *Building and Environment,* 42(1), 372-384.

Chirarattananon, S., and Hien, V. D. (2011). Thermal performance and cost effectiveness of massive walls under Thai climate. *Energy and Buildings*, 43(7), 1655-1662.

Datta, G. (2001). Effect of fixed horizontal louver shading devices on thermal performance of building by TRNSYS simulation. *Renewable Energy,* 23(3-4), 497-507.

Hammad, F., and Abu-Hijleh, B. (2010). The energy savings potential of using dynamic external louvers in an office building. *Energy and Buildings*, 42(10), 1888-1895.

Hien, V. D., and Chirarattananon, S. (2005). Triangular subdivision for the computation of form factors. *Leukos*, 2(1), 41-59.

González, J., and Fiorito, F. (2015). Daylight design of office buildings: optimisation of external solar shadings by using combined simulation methods. *Buildings*, 5(2), 560-580.

Kirimtat, A., Koyunbaba, B. K., Chatzikonstantinou, I., and Sariyildiz, S. (2016). Review of simulation modeling for shading devices in buildings. *Renewable and Sustainable Energy Reviews*, 53, 23-49.

Li, D. H. W., and Tsang, E. K. W. (2008). An analysis of daylighting performance for office buildings in Hong Kong. *Building Environment,* 43(9), 1446-1458.

Nielsen, M. V., Svendsen, S., and Jensen, L. B. (2011). Quantifying the potential of automated dynamic solar shading in office buildings through integrated simulations of energy and daylight. *Solar Energy*, 85(5), 757-768.

O'Brien, W., Kapsis, K., and Athienitis, A. K. (2013). Manually-operated window shade patterns in office buildings: A critical review. *Building Environment*, 60, 319-338.

Perez, R., Ineichen, P., Seals, R. Michalsky, J., and Stewart, R. (1990). Modeling daylight availability and irradiance components from direct and global irradiance. *Solar Energy,* 44(5), 271-289.

Stazi, F., Marinelli, S., Di Perna, C., and Munafò, P. (2014). Comparison on solar shadings: monitoring of the thermo-physical behaviour, assessment of the energy saving, thermal comfort, natural lighting and environmental impact. *Solar Energy*, 105, 512-528.

Tzempelikos, A., and Athienitis, A. K. (2007). The impact of shading design and control on building cooling and lighting demand. *Solar Energy*, 81(3), 369-382.

Yao, J., Chow, D. H. C., Zheng, R. Y., and Yan, C. W. (2016). Occupants' impact on indoor thermal comfort: A co-simulation study on stochastic control of solar shades. *Journal of Building Performance Simulation*, 9(3), 272-287.